

Kaluza-Klein Effects on Higgs Physics in Universal Extra Dimensions *

Frank J. Petriello

Stanford Linear Accelerator Center

Stanford University

Stanford CA 94309, USA

Abstract

We examine the virtual effects of Kaluza-Klein (KK) states on Higgs physics in universal extra dimension models. We study the partial widths $\Gamma_{h \rightarrow gg}$, $\Gamma_{h \rightarrow \gamma\gamma}$, and $\Gamma_{h \rightarrow \gamma Z}$, which are relevant for Higgs production and detection in future collider experiments. These interactions occur at one loop in the Standard Model, as do the KK contributions. We find that the deviations induced by the KK exchanges can be significant; for one extra dimension, the $gg \rightarrow h$ production rate is increased by 10% – 85% for the mass of the first KK state in the range $500 \gtrsim m_1 \gtrsim 1500$ GeV, a region untested by current direct search and precision measurement constraints. The $h \rightarrow \gamma\gamma$ decay width is decreased by $\lesssim 20\%$ in the same mass range. For two or more universal extra dimensions the results are cutoff dependent, and can only be qualitatively estimated. We comment on the detectability of these shifts at the LHC and at future e^+e^- and $\gamma\gamma$ colliders.

*Work supported by the Department of Energy, Contract DE-AC03-76SF00515

1 Introduction

Theories in which gravity propagates in large extra spacetime dimensions [1] have received a great deal of attention during the past several years. These models permit some of the qualitative features of string theory, such as the existence of extra dimensions and stringy resonances [2], to be tested experimentally, and predict the appearance of a wide variety of phenomenology at future high energy colliders [3]. They also furnish a solution to the hierarchy problem by lowering the fundamental Planck scale to a TeV. The string theoretic motivation for extra dimensions also allows new dimensions in which Standard Model (SM) or other non-gravitational fields can propagate [4]; for consistency with experimental constraints they must have a size of order an TeV^{-1} . Models utilizing this idea have been shown to yield a host of interesting phenomena, including TeV-scale unification [5], explanations of fermion Yukawa hierarchies [6], mechanisms for generating neutrino masses [7], and methods of rendering axions invisible [8].

One proposed scenario, referred to as the Universal Extra Dimensions (UED) model [9], allows all the SM fields to propagate in TeV^{-1} extra dimensions. At tree level, the momentum in the extra dimensions is conserved, requiring pair production of the associated Kaluza-Klein (KK) modes at colliders and preventing tree level mixing effects from altering precision electroweak measurements. The compactification scale of the UED can therefore be as low as 300 GeV for one extra dimension, and remains less than 1 TeV for two UED. The phenomenological implications of UED for collider experiments [10], $b \rightarrow s\gamma$ [11], and the muon anomalous magnetic moment [12] have been studied, and new mechanisms for generating neutrino masses [13] and suppressing proton decay [14] have been developed.

The detection of direct production of UED KK states at future colliders is expected to be difficult, for the following two reasons: (i) a remnant of extra-dimensional momentum conservation when loop effects are included implies the existence of a neutral, stable KK mode, leading to the necessity of interpreting missing energy signatures; (ii) the near degeneracy of the KK excitations within each level renders the mass shifts due to radiative corrections important in determining the pattern of decays [15]. It is therefore interesting to determine whether there are other, indirect ways in which the effects of UED can be detected. One such possibility is through the modification of Higgs production and decay processes at future colliders; determining whether such deviations can significantly modify

Higgs properties is also important considering the necessity of establishing the mechanism of electroweak symmetry-breaking. We study here the processes $gg \rightarrow h$, $h \rightarrow \gamma\gamma$, and $h \rightarrow \gamma Z$; the first interaction is the dominant Higgs production mechanism at the LHC, while the second is the primary discovery mode for $m_H \lesssim 150$ GeV. All three processes occur at one loop in the SM, the same order at which the KK excitations first contribute; we expect, and find, that these effects are quite large for the low compactification scales allowed for UED. Furthermore, graviton exchanges do not contribute to these processes at one loop, as can be seen from the unitary gauge Feynman rules in [3]. We can therefore with some sense of security neglect the gravitational effects which presumably also appear in the complete theory in which the UED are embedded [16]. We concentrate here on modifications arising from physics in UED, rather than from other extra-dimensional models, for two reasons: (i) in the Randall-Sundrum model [17] in which SM fields can propagate in the full 5-dimensional spacetime, Higgs physics is already modified at tree-level by the mixing between the Higgs and the radion field which stabilizes the extra dimension [18]; (ii) in TeV^{-1} models where only gauge fields propagate in the bulk, we expect the effects to be unobservable, because the bound on the compactification scale from electroweak precision fits is quite high [19, 20] and the top quark KK excitations which induce the majority of the effects found here are absent.

Our paper is organized as follows. In Sec. 2 we review the formulation of the SM in one additional UED, focusing on the appropriate gauge-fixing and the mixing within the top quark KK tower. We study the modifications of the processes $gg \rightarrow h$, $h \rightarrow \gamma\gamma$, and $h \rightarrow \gamma Z$ in Sec. 3; we find that the heavy KK modes decouple, yielding finite, unambiguous results for one UED. For more than one UED the sums over KK modes diverge, and only qualitative statements can be made. We find that observable modifications to Higgs production and decay processes occur for compactification masses $m_1 \lesssim 1.5$ TeV; the $gg \rightarrow h$ production rate is increased by $\approx 10\% - 85\%$ for $1500 \gtrsim m_1 \gtrsim 500$ GeV, respectively, while the decay widths are shifted by $\lesssim 20\%$ in the same interval. We present our conclusions in Sec. 4.

2 Kaluza-Klein Reduction of the 5-dimensional Standard Model

We review here the formulation of the UED model, in which all the SM fields can propagate in the extra dimensions. We restrict our attention to the 5-dimensional scenario, and focus on

the issues most pertinent to our calculation: the appropriate choice of gauge-fixing and the effects of mixing within the top quark KK tower. A detailed construction of the SM in UED is given in [9], while a discussion of generalized R_ξ gauges in a variety of extra-dimensional models is presented in [21].

We begin with the action

$$\begin{aligned}
S = & \int_{-\pi R}^{\pi R} dy \int d^4x \left\{ -\frac{1}{2} \sum_{i=1}^3 \text{Tr} [F_{iMN} F_i^{MN}] + (D_M H)^\dagger D^M H + \mu^2 |H|^2 - \frac{\lambda_5}{4} |H|^4 \right. \\
& \left. + i \bar{Q} \not{D} Q + i \bar{t} \not{D} t + [\lambda_5^t \bar{Q} i \sigma_2 H^* t + \text{h.c.}] \right\} .
\end{aligned} \tag{1}$$

Here (M, N) are the 5-dimensional Lorentz indices, and R is the radius of the fifth dimension, which we have anticipated compactifying on S^1/Z_2 . H is the Higgs doublet, and the F_i^{MN} are the field strengths for the SM gauge groups. Q is the third generation quark doublet and t is the top quark singlet; we will not need the remaining SM fermions in our analysis, and they have consequently not been included. The covariant derivative D_M can be expressed as

$$D_M = \partial_M - i \sum_{i=1}^3 g_5^i T_i^a A_{iM}^a , \tag{2}$$

where the g_5^i are the 5-dimensional coupling constants for $U(1)_Y$, $SU(2)_L$, and $SU(3)_c$, and the T_i^a are the generators of these groups. The 5-dimensional Dirac matrices are $\gamma^M = (\gamma^\mu, i \gamma^5)$. μ^2 , λ_5 , and λ_5^t are the 5-dimensional versions of the usual Higgs couplings and top quark Yukawa coupling. The parameters λ_5 , λ_5^t , and g_5^i are dimensionful, and must be rescaled to obtain the correct dimensionless SM couplings; no rescaling is necessary for the the Higgs mass parameter μ^2 .

To derive the 4-dimensional effective action we must expand the 5-dimensional fields into their KK modes; we must also remove several extra massless particles from the resulting theory. Five-dimensional fermions are necessarily vector-like, and we wish to obtain the chiral zero modes necessary for construction of the SM; this necessitates the removal of the extra zero modes appearing in the top quark KK tower. We also must eliminate the zero modes of the scalars A_i^5 that arise in the reduction of the gauge fields. To do this we follow the standard recipe of compactifying the fifth dimension on an S^1/Z_2 orbifold and requiring that the fields whose zero modes we wish to remove are odd under the orbifold projection

$y \rightarrow -y$. The appropriate KK expansions of the 5-dimensional fields are:

$$\begin{aligned}
H(x^\mu, y) &= \frac{1}{\sqrt{2\pi R}} \left\{ H^{(0)}(x^\mu) + \sqrt{2} \sum_{n=1}^{\infty} H^{(n)}(x^\mu) \cos\left(\frac{ny}{R}\right) \right\}, \\
A_{i\mu}(x^\nu, y) &= \frac{1}{\sqrt{2\pi R}} \left\{ A_{i\mu}^{(0)}(x^\nu) + \sqrt{2} \sum_{n=1}^{\infty} A_{i\mu}^{(n)}(x^\nu) \cos\left(\frac{ny}{R}\right) \right\}, \\
A_i^5(x^\nu, y) &= \frac{1}{\sqrt{\pi R}} \sum_{n=1}^{\infty} A_i^{5(n)}(x^\nu) \sin\left(\frac{ny}{R}\right), \\
Q(x^\nu, y) &= \frac{1}{\sqrt{2\pi R}} \left\{ Q_L^{(0)}(x^\nu) + \sqrt{2} \sum_{n=1}^{\infty} \left[P_L Q_L^{(n)}(x^\nu) \cos\left(\frac{ny}{R}\right) \right. \right. \\
&\quad \left. \left. + P_R Q_R^{(n)}(x^\nu) \sin\left(\frac{ny}{R}\right) \right] \right\}, \\
t(x^\nu, y) &= \frac{1}{\sqrt{2\pi R}} \left\{ t_R^{(0)}(x^\nu) + \sqrt{2} \sum_{n=1}^{\infty} \left[P_R t_R^{(n)}(x^\nu) \cos\left(\frac{ny}{R}\right) \right. \right. \\
&\quad \left. \left. + P_L t_L^{(n)}(x^\nu) \sin\left(\frac{ny}{R}\right) \right] \right\}, \tag{3}
\end{aligned}$$

where we have introduced the projection operators $P_{R,L} = (1 \pm \gamma^5)/2$. We thus obtain the desired zero modes $A_{i\mu}^{(0)}$, $Q_L^{(0)}$, and $t_R^{(0)}$, corresponding to the SM fields. These expansions should be inserted into the action of Eq. 1. We must also expand the zero mode Higgs doublet around its vev, and express the KK Higgs doublets in terms of their component fields:

$$H^{(0)} = \begin{pmatrix} \phi^{(0)+} \\ \frac{1}{\sqrt{2}} (\nu + h^{(0)} + i\chi^{(0)}) \end{pmatrix}, \quad H^{(n)} = \begin{pmatrix} \phi^{(n)+} \\ \frac{1}{\sqrt{2}} (h^{(n)} + i\chi^{(n)}) \end{pmatrix}. \tag{4}$$

Here ν is the usual 4-dimensional Higgs vev, $h^{(0)}$ is the physical zero mode Higgs, and $\chi^{(0)}$, $\phi^{\pm(0)}$ are the zero mode Goldstone bosons. The $h^{(n)}$ are the CP-even Higgs KK excitations, the $\chi^{(n)}$ are CP-odd scalars that will combine with the $Z^{5(n)}$ to form a tower of CP-odd Higgs bosons and generate the longitudinal components for the $Z_\mu^{(n)}$, and the $\phi^{\pm(n)}$ are charged scalars that together with the $W^{\pm 5(n)}$ will form a tower of charged Higgs scalars and longitudinal components for the $W_\mu^{\pm(n)}$. Inserting the expansions of Eqs. 3 and 4 into the action in Eq. 1 leads to a slew of mass terms, mixings, and couplings. We focus first on the masses and mixings in the gauge sector, introducing the appropriate gauge-fixing terms and deriving the spectrum of physical states and Goldstone fields.

We first examine the photon KK tower; the relevant mass terms and mixings are

$$S^A = \int d^4x \sum_{n=1}^{\infty} \left\{ \frac{1}{2} m_n^2 A_\mu^{(n)} A^{\mu(n)} - m_n A_\mu^{(n)} \partial^\mu A^{5(n)} \right\}, \quad (5)$$

where $m_n = n/R$ is the KK mass of the n th level arising from the derivative ∂_5 acting on the 5-dimensional wavefunctions of Eq. 3. The most natural choice of gauge-fixing is the five-dimensional analog of the Feynman gauge,

$$S_{gf}^A = -\frac{1}{2} \int_{-\pi R}^{\pi R} dy \int d^4x \left(\partial_M A^M \right)^2. \quad (6)$$

Utilizing the KK expansion of A^M , and summing Eqs. 5 and 6, we find that the mixing between $A_\mu^{(n)}$ and $A^{5(n)}$ cancels, and that we are left with the mass terms

$$S^A + S_{gf}^A = \frac{1}{2} \int d^4x \sum_{n=1}^{\infty} \left\{ m_n^2 A_\mu^{(n)} A^{\mu(n)} - m_n^2 \left(A^{5(n)} \right)^2 \right\}; \quad (7)$$

the spectrum then consists of a massless zero mode $A_\mu^{(0)}$, a tower of KK modes $A_\mu^{(n)}$ with masses m_n , and a tower of Goldstone particles $A^{5(n)}$ also with mass m_n . The treatment of the gluon KK tower proceeds identically, and we will not present it explicitly.

We next study the Z boson KK tower, together with the KK excitations of the zero mode Goldstone particle, χ . The corresponding masses and mixing terms are

$$\begin{aligned} S^Z = \frac{1}{2} \int d^4x \left\{ M_Z^2 \left(Z^{(0)} \right)^2 + 2M_Z Z_\mu^{(0)} \partial^\mu \chi^{(0)} + \sum_{n=1}^{\infty} \left[-m_n^2 \left(\chi^{(n)} \right)^2 + m_{Z,n}^2 Z_\mu^{(n)} Z^{\mu(n)} \right. \right. \\ \left. \left. - M_Z^2 \left(Z^{5(n)} \right)^2 - 2m_n M_Z Z^{5(n)} \chi^{(n)} + 2Z_\mu^{(n)} \partial^\mu \left(M_Z \chi^{(n)} - m_n Z^{5(n)} \right) \right] \right\}, \quad (8) \end{aligned}$$

where we have introduced the abbreviation $m_{Z,n}^2 = M_Z^2 + m_n^2$. We choose the straightforward 5-dimensional generalization of the usual SM Feynman gauge,

$$S_{gf}^Z = -\frac{1}{2} \int_{-\pi R}^{\pi R} dy \int d^4x \left(\partial_M Z^M - M_Z \chi \right)^2; \quad (9)$$

utilizing the KK expansion of Eq. 3 and combining this with Eq. 8, we derive the following mass terms:

$$\begin{aligned} S^Z + S_{gf}^Z = \frac{1}{2} \int d^4x \left\{ M_Z^2 Z_\mu^{(0)} Z^{\mu(0)} - M_Z^2 \left(\chi^{(0)} \right)^2 + \sum_{n=1}^{\infty} \left[m_{Z,n}^2 Z_\mu^{(n)} Z^{\mu(n)} \right. \right. \\ \left. \left. - m_{Z,n}^2 \left(\chi^{(n)} \right)^2 - m_{Z,n}^2 \left(Z^{5(n)} \right)^2 \right] \right\}; \quad (10) \end{aligned}$$

the mixing between $Z_\mu^{(n)}$ and $Z^{5(n)}$ cancels. It is clear from Eq. 8 that the linear combinations of fields that serve as Goldstone modes for the Z boson KK tower are

$$G_Z^{(n)} = \frac{M_Z \chi^{(n)} - m_n Z^{5(n)}}{\sqrt{M_Z^2 + m_n^2}}, \quad (11)$$

while the physical CP-odd scalars are

$$\chi_Z^{(n)} = \frac{m_n \chi^{(n)} + M_Z Z^{5(n)}}{\sqrt{M_Z^2 + m_n^2}}. \quad (12)$$

With the gauge choice we have made, the states $G_Z^{(n)}$, $\chi_Z^{(n)}$, and $Z_\mu^{(n)}$ all possess the mass $m_{Z,n}$.

Finally, we consider the masses and mixing terms involving the W^\pm KK tower and the KK excitations of the zero mode Goldstone fields ϕ^\pm :

$$\begin{aligned} S^W = & \int d^4x \left\{ M_W^2 W_\mu^{+(0)} W^{-\mu(0)} + iM_W \left(W_\mu^{-(0)} \partial^\mu \phi^{+(0)} - W_\mu^{+(0)} \partial^\mu \phi^{-(0)} \right) \right. \\ & + \sum_{n=1}^{\infty} \left[-m_n^2 \phi^{+(n)} \phi^{-(n)} + m_{W,n}^2 W_\mu^{+(n)} W^{-\mu(n)} - M_W^2 W^{+5(n)} W^{-5(n)} \right. \\ & - im_n M_W \left(W^{-5(n)} \phi^{+(n)} - W^{+5(n)} \phi^{-(n)} \right) - W_\mu^{-(n)} \partial^\mu \left(m_n W^{+5(n)} - iM_W \phi^{+(n)} \right) \\ & \left. \left. - W_\mu^{+(n)} \partial^\mu \left(m_n W^{-5(n)} + iM_W \phi^{-(n)} \right) \right] \right\}, \quad (13) \end{aligned}$$

where we have abbreviated $m_{W,n}^2 = M_W^2 + m_n^2$. The appropriate choice of gauge-fixing term is again the obvious 5-dimensional extension of the SM Feynman gauge:

$$S_{gf}^W = - \int_{-\pi R}^{\pi R} dy \int d^4x \left(\partial_M W^{+M} - iM_W \phi^+ \right) \left(\partial_M W^{-M} + iM_W \phi^- \right). \quad (14)$$

Inserting the KK expansions of Eq. 3 into this expression, and adding it to Eq. 13, we find that the mixing between $W_\mu^{\pm(n)}$ and $W^{\pm 5(n)}$ cancels, and we obtain the mass terms

$$\begin{aligned} S^W + S_{gf}^W = & \int d^4x \left\{ M_W^2 W_\mu^{+(0)} W^{-\mu(0)} - M_W^2 \phi^{+(0)} \phi^{-(0)} \right. \\ & \left. + \sum_{n=1}^{\infty} \left[m_{W,n}^2 W_\mu^{+(n)} W^{-\mu(n)} - m_{W,n}^2 W^{+5(n)} W^{-5(n)} - m_{W,n}^2 \phi^{+(n)} \phi^{-(n)} \right] \right\}. \quad (15) \end{aligned}$$

Again, the Goldstone modes are linear combinations of the 5-dimensional components of the gauge fields, $W^{\pm 5(n)}$, and the KK excitations of the zero mode Goldstone, $\phi^{\pm(n)}$:

$$G^{\pm(n)} = \frac{m_n W^{\pm 5(n)} \mp i M_W \phi^{\pm(n)}}{\sqrt{m_n^2 + M_W^2}} . \quad (16)$$

The physical charged Higgs pair is the orthogonal combination:

$$H^{\pm(n)} = \frac{m_n \phi^{\pm(n)} \mp i M_W W^{\pm 5(n)}}{\sqrt{m_n^2 + M_W^2}} . \quad (17)$$

In the 5-dimensional generalization of the SM Feynman gauge we employ, the fields $W^{\pm\mu(n)}$, $G^{\pm(n)}$, and $H^{\pm(n)}$ share the common mass $m_{W,n}$.

Having computed the spectrum of states in the gauge sector, we can now derive the interactions of the gauge and scalar particles; we identify the 4-dimensional couplings as $\lambda = \lambda_5/2\pi R$, $\lambda^t = \lambda_5^t/\sqrt{2\pi R}$, and $g^i = g_5^i/\sqrt{2\pi R}$ so that the zero mode interactions match those of the SM. Letting $\phi_i^{(n)}$ denote a KK excitation of an arbitrary SM field, the contributing KK interactions take the form

$$\phi_i^{(0)} \phi_j^{(n)} \phi_k^{(n)} , \quad \phi_i^{(0)} \phi_j^{(0)} \phi_k^{(n)} \phi_l^{(n)} . \quad (18)$$

The explicit expressions for these vertices are simple to obtain; for every SM vertex $\phi_i^{(0)} \phi_j^{(0)} \phi_k^{(0)}$ or $\phi_i^{(0)} \phi_j^{(0)} \phi_k^{(0)} \phi_l^{(0)}$, there is a corresponding KK vertex with exactly the same coupling strength. We note explicitly that the $h^{(0)} W^{+(n)} W^{-(n)}$ and $h^{(0)} Z^{(n)} Z^{(n)}$ vertices are identical to the $h^{(0)} W^{+(0)} W^{-(0)}$ and $h^{(0)} Z^{(0)} Z^{(0)}$ vertices; the masses that appear in the KK interactions are M_W and M_Z , not $m_{W,n}$ and $m_{Z,n}$. The heavy KK states decouple from the processes considered here, allowing us to obtain finite results in five dimensions when the sum over KK modes is performed. The only other interactions needed for our calculation are those involving $W^{\pm 5(n)}$; these are given in the appendix. For a complete list of the SM vertices we refer the reader to [22]; we will not reproduce them here.

We now derive the interactions of the top quark KK states required in our analysis. Although there is no mixing between different levels of the top quark KK tower, the doublet and singlet states within each level mix. The mass matrix for the n th KK level arising from

the reduction of Eq. 1 is

$$\left(\bar{Q}_L^{(n)}, \bar{t}_L^{(n)}\right) \begin{pmatrix} m_n & m_t \\ m_t & -m_n \end{pmatrix} \begin{pmatrix} Q_R^{(n)} \\ t_R^{(n)} \end{pmatrix} + \text{h.c.}, \quad (19)$$

where m_t is the zero mode top quark mass. This can be diagonalized with the following unitary matrices for the left and right-handed fields:

$$U_L^{(n)} = \begin{pmatrix} \cos(\alpha^{(n)}/2) & \sin(\alpha^{(n)}/2) \\ \sin(\alpha^{(n)}/2) & -\cos(\alpha^{(n)}/2) \end{pmatrix}, \quad U_R^{(n)} = \begin{pmatrix} \cos(\alpha^{(n)}/2) & \sin(\alpha^{(n)}/2) \\ -\sin(\alpha^{(n)}/2) & \cos(\alpha^{(n)}/2) \end{pmatrix}, \quad (20)$$

where both states in the physical basis have mass $m_{t,n} = \sqrt{m_n^2 + m_t^2}$, and $\cos(\alpha^{(n)}) = m_n/m_{t,n}$, $\sin(\alpha^{(n)}) = m_t/m_{t,n}$. We must derive the couplings of these states to $h^{(0)}$, $A_\mu^{(0)}$, $Z_\mu^{(0)}$, and $g_\mu^{(0)}$ for our analysis. Denoting the mass eigenbasis of the n th level by the vector $T^{(n)}$, we find the following KK interactions:

$$S^t = \int d^4x \sum_{n=1}^{\infty} \left\{ \bar{T}^{(n)} A^{(0)} C_A^{(n)} T^{(n)} + \bar{T}^{(n)} Z^{(0)} C_{Z,V}^{(n)} T^{(n)} + \bar{T}^{(n)} g^{(0)} C_g^{(n)} T^{(n)} \right. \\ \left. + \left[h^{(0)} \bar{T}^{(n)} C_h^{(n)} T^{(n)} + \text{h.c.} \right] \right\}. \quad (21)$$

The coupling matrices appearing in this expression are

$$C_A^{(n)} = eQ_t \begin{pmatrix} 1 & 0 \\ 0 & 1 \end{pmatrix}, \quad C_{Z,V}^{(n)} = \frac{g}{c_W} \begin{pmatrix} g_v - g_a \cos(\alpha^{(n)}) & 0 \\ 0 & g_v + g_a \cos(\alpha^{(n)}) \end{pmatrix} \\ C_h^{(n)} = m_t \begin{pmatrix} \sin(\alpha^{(n)}) & \cos(\alpha^{(n)}) \\ -\cos(\alpha^{(n)}) & \sin(\alpha^{(n)}) \end{pmatrix}, \quad C_g^{(n)} = g_3 \begin{pmatrix} 1 & 0 \\ 0 & 1 \end{pmatrix}, \quad (22)$$

where Q_t is the top quark charge in units of e , c_W is the cosine of the weak mixing angle, g and g_3 are respectively the coupling constants of $SU(2)_L$ and $SU(3)_c$, and g_v, g_a are the top quark vector and axial couplings to the SM Z . The γ^5 component of the Z interaction does not contribute to the studied processes, and has consequently not been included. We note that the coupling of top quark KK states to the Higgs is proportional to m_t , not $m_{t,n}$; the

heavy KK top quarks decouple as do the $W^{\pm(n)}$ and $Z^{(n)}$ towers. This is in contrast to the behavior of a heavy fourth generation quark, whose coupling to the Higgs is proportional to its mass, and which does not decouple.

We now possess the tools required to study corrections to Higgs boson production and decay processes arising from one loop KK exchanges. We will concentrate on the processes $gg \rightarrow h$, $h \rightarrow \gamma\gamma$, and $h \rightarrow \gamma Z$, which occur at one loop in the SM; the KK contributions to these interactions are therefore of the same order as the SM contributions. The decoupling of the higher KK modes allows us to obtain finite predictions when only one extra dimension is considered; furthermore, at one loop graviton exchanges do not contribute to these processes, rendering our neglect of the gravity sector of the theory justifiable. These features allow us to obtain unambiguous and testable predictions.

3 KK Effects in One Loop Higgs Processes

We now study the effects of virtual KK exchanges in $gg \rightarrow h$, $h \rightarrow \gamma\gamma$, and $h \rightarrow \gamma Z$, processes relevant for Higgs production and decay at the LHC. Both the SM and KK contributions to these interactions occur at one loop, and we therefore expect the modifications arising from KK exchanges to be significant. This is indeed the case; we will find that KK effects are visible for the compactification mass m_1 in the range $400 \text{ GeV} \lesssim m_1 \lesssim 1500 \text{ GeV}$, a region consistent with the constraints arising from both direct searches and precision measurements [9].

3.1 $gg \rightarrow h$

The process $gg \rightarrow h$ proceeds in the SM through diagrams containing fermion triangle loops. We consider only contributions arising from the top quark and its KK tower; the couplings of other fermions to the Higgs are much smaller than that of the top quark, and are negligible in our analysis. The production cross section, which is proportional to the $h \rightarrow gg$ width, can be written in the form

$$\sigma_{gg \rightarrow h} = \frac{G_F [\alpha_s(m_H)]^2}{32\sqrt{2}\pi m_H^4} |F_t|^2, \quad (23)$$

where G_F is the Fermi constant, $\alpha_s(m_H)$ is the QCD coupling strength evaluated at the Higgs mass scale, and F_t is the contribution of the loop integrals over the top quark KK

tower contributions. Introducing the abbreviation

$$C_0(m^2) = C_0(m_H^2, 0, 0; m^2, m^2, m^2) \quad (24)$$

for the three-point scalar Passarino-Veltman function [23, 22], the SM result becomes

$$F_t^{SM} = -2m_t^2 + m_t^2 (m_H^2 - 4m_t^2) C_0(m_t^2) . \quad (25)$$

The scalar three-point function of Eq. 24 can be evaluated in terms of elementary functions, yielding

$$C_0(m^2) = \begin{cases} -\frac{2}{m_H^2} \left[\arcsin \left(\frac{1}{\sqrt{\tau}} \right) \right]^2 & \tau \geq 1 \\ \frac{1}{2m_H^2} \left[\ln \left(\frac{1+\sqrt{1-\tau}}{1-\sqrt{1-\tau}} \right) - i\pi \right]^2 & \tau < 1 \end{cases} , \quad (26)$$

where $\tau = 4m^2/m_H^2$. The couplings of the top quark KK excitations to both zero mode Higgs bosons and photons are given in Eq. 22; utilizing these expressions, we can write $F_t = F_t^{SM} + F_t^{KK}$, where

$$F_t^{KK} = 2m_t \sum_{n=1}^{\infty} m_{t,n} \sin(\alpha^{(n)}) \left\{ -2 + (m_H^2 - 4m_{t,n}^2) C_0(m_{t,n}^2) \right\} . \quad (27)$$

In obtaining this formula, and other formulae presented in this paper, we used QGRAF [28] to check that we included all the appropriate diagrams and FORM [29] to verify our algebraic manipulations. In the limit $m^2 \rightarrow \infty$, $C_0(m^2) \approx -1/2m^2 - m_H^2/24m^4$. Applying this result to F_t^{KK} , we find that

$$F_t^{KK} \approx -\frac{2m_H^2 m_t^2}{3} \sum_{n=1}^{\infty} \frac{1}{m_n^2} \quad (28)$$

in the limit that the KK mass parameters m_n are much larger than either m_t or m_H . In five dimensions this sum is over a single index n , and we obtain a convergent result. In greater than five dimensions we must sum over an array of indices n_i , where i ranges over the number of extra dimensions, and F_t^{KK} diverges (in more than five dimensions there is also a greater multiplicity of states arising from the KK reduction [24], which affects both the finite piece and the coefficient of the divergent part of the sum). These divergent sums can be evaluated by introducing a cutoff Λ ; in six dimensions, for example, this leads to the

result $F_t^{KK} \propto \ln(\Lambda R)$. We will not study scenarios with $D > 5$ here; we expect, however, that the results we obtain in the 5-dimensional case will be qualitatively similar to those found in the complete $D > 5$ theory in which these UED are embedded, and in which this arbitrariness is removed.

Since the lower bound on the KK mass parameter m_1 in UED models is quite low, $m_1 \gtrsim 300 - 400$ GeV, we expect the deviations due to the virtual KK exchanges to be large. We present in Fig. 1 the fractional deviation of the production cross section from that of the SM for the following choices of compactification mass: $m_1 = 500, 750, 1000, 1250, 1500$ GeV. It was argued in [9] that the 4-dimensional effective theory remains valid until $m_n \approx 10$ TeV. A negligible fraction of the effects found here are induced by KK modes with masses above this value, and we can therefore trust our results for the compactification masses $m_1 \leq 1.5$ TeV considered. Fits to the electroweak precision data within the framework of extra-dimensional models typically allow Higgs masses larger than the 95% CL upper bound obtained in the SM [20]; we therefore present results for the range $m_H \leq 500$ GeV. For $m_1 = 500$ GeV and $m_H \approx 120$ GeV, the production rate is $\approx 85\%$ larger than in the SM; this decreases to 40% for a 500 GeV Higgs. For $m_1 = 1500$ GeV and $m_H \approx 120$ GeV the increase is $\approx 10\%$. A more complete analysis would take into account the next-to-leading order QCD corrections, which significantly increase $\sigma_{gg \rightarrow h}$ [25], and the next-to-next-to-leading order QCD corrections in the $m_t \rightarrow \infty$ limit, which have recently been computed [26]. However, the KK contributions will receive the same QCD corrections, and we expect that for $m_1 \lesssim 1.5$ TeV and a light Higgs boson, deviations arising from physics in UED should be observable. Future e^+e^- linear colliders will determine the $h \rightarrow gg$ decay width with a 10% – 12.5% precision for Higgs masses in the range 120 – 140 GeV [27], indicating that compactification masses $m_1 \lesssim 1500$ GeV are indeed testable.

We will examine the observability of UED contributions at future colliders in more detail in the following subsections, where we compute the corresponding deviations arising from KK exchanges in the decays $h \rightarrow \gamma\gamma$ and $h \rightarrow \gamma Z$. This will allow us to estimate the total shift in production rates for the processes $gg \rightarrow \gamma\gamma, \gamma Z$, which are relevant for Higgs searches at the LHC.

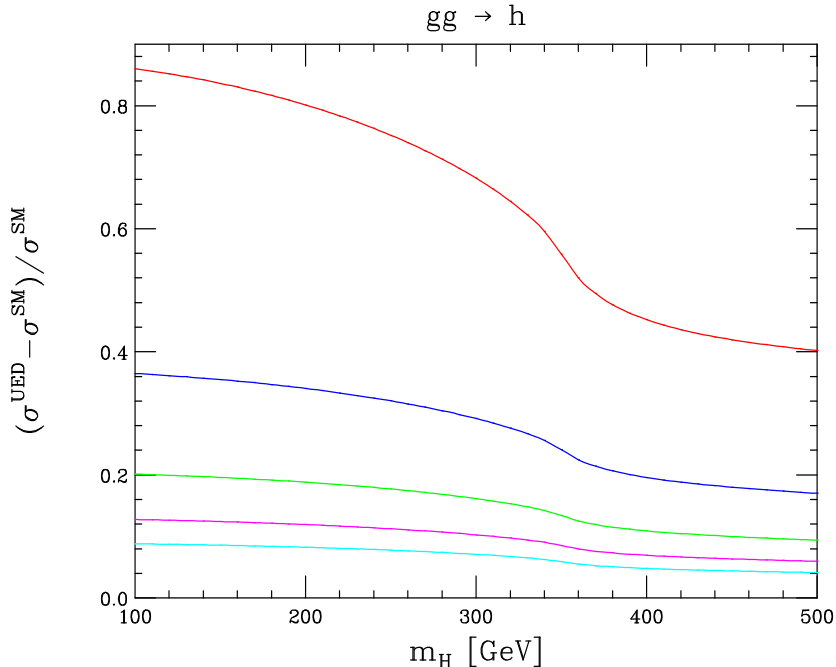


Figure 1: The fractional deviation of the $gg \rightarrow h$ production rate in the UED model as a function of m_H ; from top to bottom, the results are for $m_1 = 500, 750, 1000, 1250, 1500$ GeV.

3.2 $h \rightarrow \gamma\gamma$

We now study the decay $h \rightarrow \gamma\gamma$, which is the primary discovery mode at the LHC for a Higgs with mass $m_H \lesssim 150$ GeV. At one loop, this process proceeds through both top quark and gauge sector loops, with the latter involving the W^\pm tower and its associated Goldstone modes and ghosts. The decay width can be written as

$$\Gamma_{h \rightarrow \gamma\gamma} = \frac{G_F \alpha^2}{8\sqrt{2}\pi^3 m_H} |F|^2, \quad (29)$$

where α is the electromagnetic coupling, and $F = F_W + 3Q_t^2 F_t$. The SM result for F_t^{SM} is given in Eq. 25, and

$$F_W^{SM} = \frac{1}{2} m_H^2 + 3M_W^2 - 3M_W^2 (m_H^2 - 2M_W^2) C_0(M_W^2). \quad (30)$$

In the UED model there are additional contributions from the top quark KK tower, the W^\pm tower and its associated Goldstone modes, ghost KK states, and the H^\pm tower defined in Eq. 17. We set $F_t = F_t^{SM} + F_t^{KK}$ and $F_W = F_W^{SM} + F_G^{KK}$, with F_t^{KK} denoting the top quark

KK tower contribution and F_G^{KK} including the contributions of the KK excitations in the gauge and Higgs sectors. F_t^{KK} is then given by the expression in Eq. 27, and

$$F_G^{KK} = \sum_{n=1}^{\infty} \left\{ \frac{1}{2} m_H^2 + 4M_W^2 - \left[4M_W^2 (m_H^2 - 2m_{W,n}^2) - m_H^2 m_{W,n}^2 \right] C_0(m_{W,n}^2) \right\}. \quad (31)$$

Using the expansion $C_0(m^2) \approx -1/2m^2 - m_H^2/24m^4$, it is simple to check that this sum converges in five dimensions. However, it diverges for $D > 5$, as does the $gg \rightarrow h$ production cross section. We again expect that the results we obtain will be qualitatively similar for $D > 5$ when the cutoff dependence is fixed by a more complete theory.

The interference between the SM and KK contributions is more intricate in $h \rightarrow \gamma\gamma$ than in $gg \rightarrow h$, as thresholds exist at both $2M_W$ and $2m_t$ where the relative importance of the various contributions can change. The fractional deviation of the $h \rightarrow \gamma\gamma$ decay width is shown in Fig. 2 for five choices of m_1 , and the fractional deviations due to the top quark KK tower and the gauge and Higgs tower contributions are presented separately for $m_1 = 500$ GeV in Fig. 3. The $\gamma\gamma$ decay width in the UED model is $\approx 12\%$ smaller than in the SM for $m_H \lesssim 2M_W$ and $m_1 = 500$ GeV, the Higgs mass region in which this decay is expected to be the discovery mode at the LHC; this result drops to $\approx 4\%$ for $m_1 = 1000$ GeV. However, at $m_H \approx 2m_t$ the decay width in the UED scenario becomes larger than in the SM. The relevant contributions of the top quark and gauge sector KK towers are shown in Fig. 3. The contribution of the top quark KK tower, the dominant UED term, interferes destructively with the SM result below the $2m_t$ threshold; this behavior reverses above threshold.

To determine the sensitivity of the LHC to these effects, we must compute the net shift in the $\gamma\gamma$ production rate resulting from the deviations in both $gg \rightarrow h$ and $h \rightarrow \gamma\gamma$. For resonant production of the Higgs, the $\gamma\gamma$ signal is well approximated by taking $\sigma_{gg \rightarrow h} \times \Gamma_{h \rightarrow \gamma\gamma}$, including the parton density functions evaluated at the relevant scale, and multiplying by the appropriate prefactors. The fractional deviation in the $\gamma\gamma$ production rate is presented in Fig. 4 for five choices of m_1 . For $m_H \lesssim 150$ GeV, the region of interest at the LHC, the increase in $\sigma_{gg \rightarrow h}$ and the decrease in $\Gamma_{h \rightarrow \gamma\gamma}$ yield a total $\approx 10\% - 65\%$ increase in the total rate as m_1 is varied from 1250 GeV to 500 GeV, respectively. The LHC is expected to be sensitive to this rate at the 10% – 15% level [30]; consequently, we expect signals from UED to be visible if $m_1 \lesssim 1000 - 1250$ GeV. An independent measurement of the $h \rightarrow \gamma\gamma$ decay width will be achievable at future linear colliders; for $m_h \lesssim 150$ GeV, a measurement of the $h\gamma\gamma$ coupling at the 7% – 10% level will be possible [27]. This will provide a test of UED

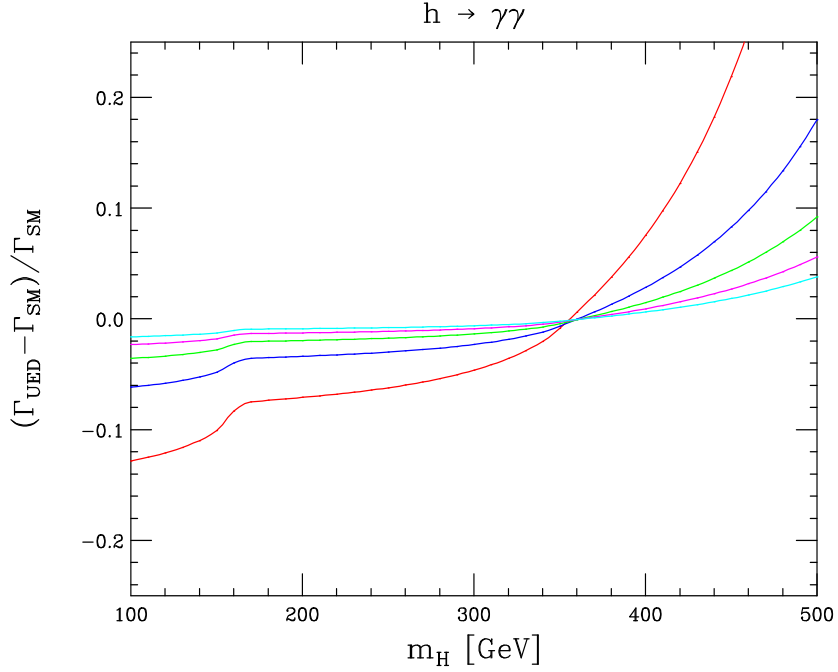


Figure 2: The fractional deviation of the $h \rightarrow \gamma\gamma$ decay width in the UED model as a function of m_H ; from top to bottom on the right, the results are for $m_1 = 500, 750, 1000, 1250, 1500$ GeV.

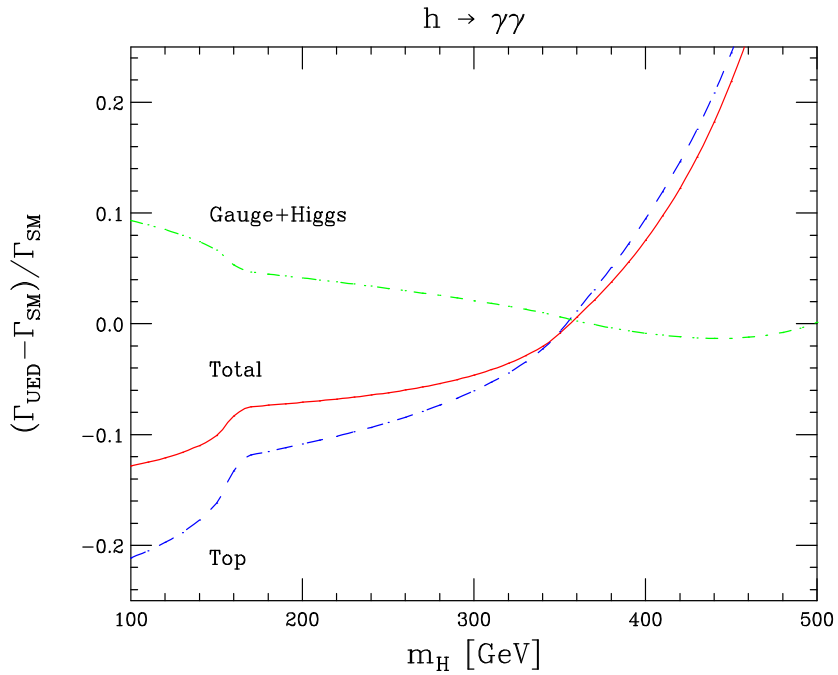


Figure 3: The fractional deviation of the $h \rightarrow \gamma\gamma$ decay width for $m_1 = 500$ GeV as a function of m_H , with the contributions of the top quark sector and the gauge and Higgs sectors shown separately.

models with $m_1 \lesssim 800$ GeV. A measurement of the $h \rightarrow \gamma\gamma$ width with an accuracy of $\approx 2\%$ is possible with the proposed photon collider option of future e^+e^- colliders [31]; this would allow probes of the UED model with KK mass parameter $m_1 \lesssim 1500$ GeV.

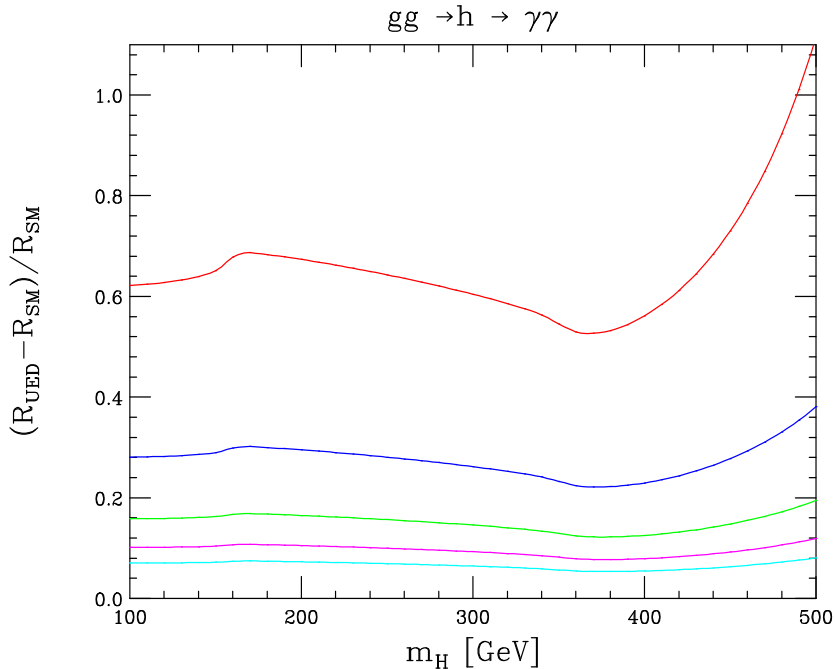


Figure 4: The fractional deviation of $R = \sigma_{gg \rightarrow h} \times \Gamma_{h \rightarrow \gamma\gamma}$, the $\gamma\gamma$ production rate, in the UED model as a function of m_H ; from top to bottom, the results are for $m_1 = 500, 750, 1000, 1250, 1500$ GeV.

3.3 $h \rightarrow \gamma Z$

We examine here the decay $h \rightarrow \gamma Z$, which proceeds in the SM through top quark and gauge sector loops. Although the width of this process exceeds the $h \rightarrow \gamma\gamma$ width for Higgs masses in the range $m_H \gtrsim 130$ GeV, the single photon and need to demand a leptonic Z decay for reconstruction purposes render it less interesting at the LHC. However, since it potentially provides another test of the detailed properties of the Higgs boson, we study modifications of this decay arising from physics in UED.

The decay width can be expressed as

$$\Gamma_{h \rightarrow \gamma Z} = \frac{\alpha G_F^2 M_W^2 m_H^3 s_W^2}{64\pi^4} \left(1 - \frac{M_Z^2}{m_H^2}\right)^3 |F|^2, \quad (32)$$

where s_W is the sine of the weak mixing angle. We introduce the abbreviation

$$\begin{aligned} C_2(m^2) &= C_1(m_H^2, M_Z^2, 0; m^2, m^2, m^2) + C_{11}(m_H^2, M_Z^2, 0; m^2, m^2, m^2) \\ &\quad + C_{12}(m_H^2, M_Z^2, 0; m^2, m^2, m^2), \end{aligned} \quad (33)$$

where C_1 , C_{11} , and C_{12} are the Passarino-Veltman tensor coefficients defined in [22], and change slightly our shorthand notation for the scalar three-point function:

$$C_0(m^2) = C_0(m_H^2, M_Z^2, 0; m^2, m^2, m^2). \quad (34)$$

These can be evaluated in terms of elementary functions [32]; setting $\tau_Z = 4m^2/M_Z^2$ and $\tau_H = 4m^2/m_H^2$, we have

$$\begin{aligned} 4m^2 C_2(m^2) &= \frac{\tau_Z \tau_H}{2(\tau_Z - \tau_H)} + \frac{\tau_Z \tau_H^2}{2(\tau_Z - \tau_H)^2} \{ \tau_Z [f(\tau_Z) - f(\tau_H)] + 2 [g(\tau_Z) - g(\tau_H)] \}, \\ 4m^2 C_0(m^2) &= \frac{2\tau_Z \tau_H}{\tau_Z - \tau_H} [f(\tau_Z) - f(\tau_H)], \end{aligned} \quad (35)$$

where

$$f(\tau) = \begin{cases} \left[\arcsin\left(\frac{1}{\sqrt{\tau}}\right) \right]^2 & \tau \geq 1 \\ -\frac{1}{4} \left[\ln\left(\frac{1+\sqrt{1-\tau}}{1-\sqrt{1-\tau}}\right) - i\pi \right]^2 & \tau < 1 \end{cases}, \quad (36)$$

and

$$g(\tau) = \begin{cases} \sqrt{\tau-1} \arcsin\left(\frac{1}{\sqrt{\tau}}\right) & \tau \geq 1 \\ \frac{1}{2} \sqrt{1-\tau} \left[\ln\left(\frac{1+\sqrt{1-\tau}}{1-\sqrt{1-\tau}}\right) - i\pi \right] & \tau < 1 \end{cases}. \quad (37)$$

Writing

$$F = \cot(\theta_W) F_W + 3 \frac{g_v Q_t}{s_W c_W} F_t, \quad (38)$$

where θ_W is the weak mixing angle, the SM result becomes

$$\begin{aligned}
F_t^{SM} &= 4m_t^2 \{4C_2(m_t^2) + C_0(m_t^2)\} \\
F_W^{SM} &= 4 \left\{ -M_W^2 (3C_0(M_W^2) + 5C_2(M_W^2)) - \frac{1}{2}m_H^2 C_0(M_W^2) \right. \\
&\quad \left. + s_W^2 [M_W^2 (6C_2(M_W^2) + 4C_0(M_W^2)) + m_H^2 C_2(M_W^2)] \right\}. \tag{39}
\end{aligned}$$

In our notation, $g_v = I_3/2 - s_W^2 Q_t$, where I_3 is the third component of the top quark weak isospin. In the UED model, there are additional contributions from both the top quark KK tower and the gauge sector KK excitations; partitioning these pieces as in the $h \rightarrow \gamma\gamma$ case, $F_t = F_t^{SM} + F_t^{KK}$ and $F_W = F_W^{SM} + F_G^{KK}$, we find

$$\begin{aligned}
F_t^{KK} &= 8 \sum_{n=1}^{\infty} \left\{ m_t m_{t,n} \sin(\alpha^{(n)}) [4C_2(m_{t,n}^2) + C_0(m_{t,n}^2)] \right\} \\
F_G^{KK} &= 4 \sum_{n=1}^{\infty} \left\{ -M_W^2 (3C_0(M_W^2) + 7C_2(M_W^2)) - \frac{1}{2}m_H^2 C_0(M_W^2) \right. \\
&\quad \left. + s_W^2 [M_W^2 (8C_2(M_W^2) + 4C_0(M_W^2)) + m_H^2 C_2(M_W^2)] \right\}. \tag{40}
\end{aligned}$$

We have used the couplings given in Eq. 22 in deriving these results. It can be checked that these sums converge in $D = 5$, but diverge for $D > 5$; again, we concentrate on the $D = 5$ scenario.

We present the fractional deviation of $\Gamma_{h \rightarrow \gamma Z}$ in the UED model in Fig. 5 for five choices of the KK mass parameter m_1 , and show the relative contributions of the top quark and gauge sectors in Fig. 6. The decay width in the UED model is slightly larger than the SM width for $m_H \lesssim 275$ GeV, and slightly smaller for higher values of m_H . The top quark and gauge sector KK towers have contributions with approximately equal magnitude but opposite sign, as seen in Fig. 6, and their effects tend to cancel. For all m_H and m_1 considered the deviation is $\lesssim 10\%$, and is hence smaller than the modifications to the gg and $\gamma\gamma$ widths. An effect of this magnitude is possibly observable at future linear colliders, although a detailed analysis of this decay mode has not been performed; it is also possible that such an effect could be observed in the $\gamma\gamma$ collision option of future colliders.

The fractional deviation of the γZ production rate at the LHC via $gg \rightarrow h \rightarrow \gamma Z$ is shown in Fig. 7 for five choices of m_H . The production increase is $\approx 95\%$ for $m_H \lesssim 150$ GeV

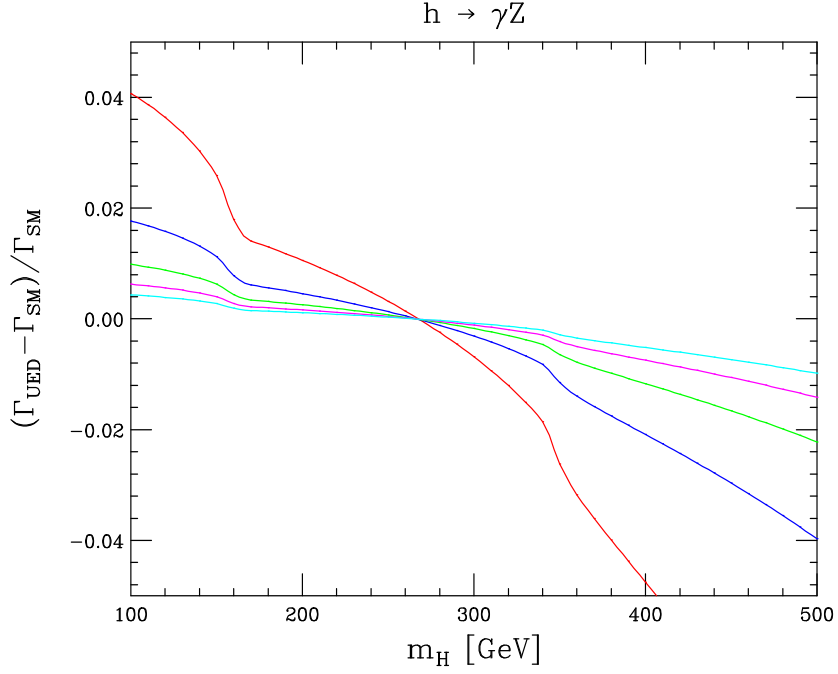


Figure 5: The fractional deviation of the $h \rightarrow \gamma Z$ decay width in the UED model as a function of m_H ; from top to bottom on the left, the results are for $m_1 = 500, 750, 1000, 1250, 1500$ GeV.

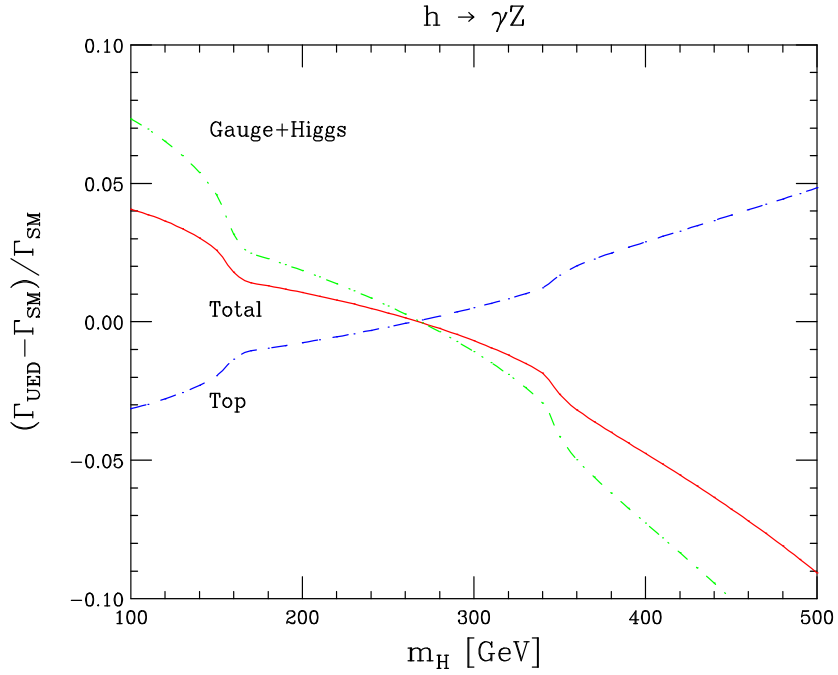


Figure 6: The fractional deviation of the $h \rightarrow \gamma Z$ decay width for $m_1 = 500$ GeV as a function of m_H , with the contributions of the top quark sector and the gauge and Higgs sectors shown separately.

and $m_1 = 500$ GeV, and $\approx 20\%$ for $m_1 = 1000$ GeV. This shift is caused primarily by the $gg \rightarrow h$ deviation; however, it may render this decay mode visible above the background at the LHC. Again, a detailed analysis of this decay at the LHC has not been performed.

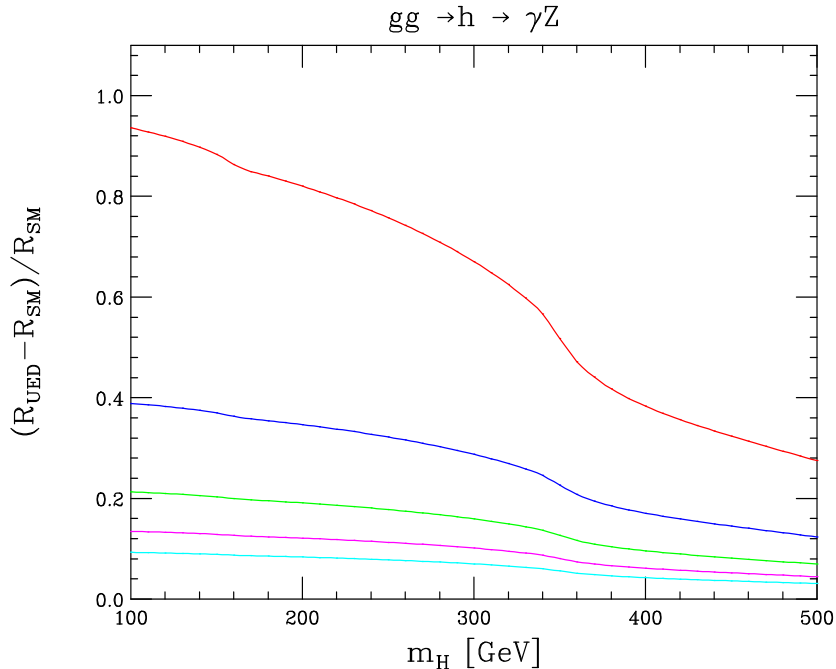


Figure 7: The fractional deviation of $R = \sigma_{gg \rightarrow h} \times \Gamma_{h \rightarrow \gamma Z}$, the γZ production rate, in the UED model as a function of m_H ; from top to bottom, the results are for $m_1 = 500, 750, 1000, 1250, 1500$ GeV.

4 Conclusions

We have studied the virtual effects of KK excitations in UED on Higgs production and decay processes relevant for high energy experiments at the LHC and at future linear colliders. The heavy KK modes decouple, allowing us to obtain unambiguous predictions for one extra dimension. For two or more extra dimensions the KK mode sums diverge, and while we expect our results in these scenarios to be qualitatively similar to those obtained here, we cannot make precise predictions. We have found that the KK excitation contributions can be quite significant; the $gg \rightarrow h$ production rate can be $\approx 85\%$ larger than the SM result for $m_H \lesssim 150$ GeV and KK mass parameter $m_1 = 500$ GeV, a value allowed by current

constraints. For $m_1 \approx 1500$ GeV, the rate increase is $\approx 10\%$; assuming the SM theoretical prediction is under control by the time the LHC turns on, this should be an observable shift. The corresponding deviations in the $h \rightarrow gg$ decay width can be probed at future e^+e^- colliders, allowing compactification masses in the range $m_1 \lesssim 1500$ GeV to be tested. The width of the decay $h \rightarrow \gamma\gamma$, the primary discovery mode for a Higgs with mass $m_H \lesssim 150$ GeV at the LHC, is decreased relative to the SM prediction by $\approx 12\%$. The total $\gamma\gamma$ production rate is increased by $\approx 10\% - 65\%$ for $1250 \gtrsim m_1 \gtrsim 500$ GeV when the reaction $gg \rightarrow h \rightarrow \gamma\gamma$ relevant at the LHC is considered. With the $10\% - 15\%$ accuracy expected in the determination of this rate at the LHC, compactification masses $m_1 \lesssim 1250$ GeV can be probed. The $h \rightarrow \gamma\gamma$ width can be independently measured at future e^+e^- and $\gamma\gamma$ colliders; we expect the effects from compactification masses $m_1 \lesssim 800$ GeV to be observable with the $7\% - 10\%$ precision expected at e^+e^- colliders, and from masses $m_1 \lesssim 1500$ GeV to be testable with the 2% precision expected at $\gamma\gamma$ colliders. Finally, we have examined the deviations in the decay $h \rightarrow \gamma Z$ predicted by UED models. We have found that the deviations from the SM result are less than $\approx 10\%$ throughout the m_H, m_1 region studied. However, the process $gg \rightarrow h \rightarrow \gamma Z$ is expected to increase by $\approx 20\% - 95\%$ for compactification masses in the range $1000 \gtrsim m_1 \gtrsim 500$ GeV. No detailed study of this process has been performed for either the LHC or future linear colliders; however, the production increase at the LHC is possibly visible above background.

How do these results compare with the deviations induced in other new physics models? In the Randall-Sundrum model studied in [18], where the Higgs and radion fields mix, both $\Gamma_{h \rightarrow gg}$ and $\Gamma_{h \rightarrow \gamma\gamma}$ are decreased throughout the allowed parameter space; the total Higgs production rate can be decreased to $\lesssim 1\%$ of the SM value for a large range of Higgs-radion mixing strengths. These results for $\Gamma_{h \rightarrow gg}$ are the opposite of those found here, in which the width is increased throughout the allowed parameter space. The situation is murkier in the Minimal Supersymmetric Standard Model (MSSM), as a large number of parameters enter calculations at the one loop level. A detailed study of Higgs physics in the MSSM was performed in [33]. Typically, $\Gamma_{h \rightarrow gg}$ is decreased by $\lesssim 15\%$ throughout the allowed parameter space, while $\Gamma_{h \rightarrow \gamma\gamma}$ is shifted by $\lesssim 5\%$, with the direction of the shift parameter dependent. Again, the deviation in $\Gamma_{h \rightarrow gg}$ is opposite that found here. $\Gamma_{h \rightarrow gg}$ was also studied in [34] within a supersymmetric extra-dimensional scenario [35]. In this model, $\Gamma_{h \rightarrow gg}$ receives contributions from loops of both top and stop KK excitations; the localization of fermion Yukawa couplings at orbifold fixed points induces mixing within these KK towers.

The width is decreased relative to its SM value throughout the entire parameter space; for a Higgs with $m_H \approx 120$ GeV the width is $\lesssim 25\%$ of the SM result. This is again opposite the shift found here. The effects of any of these scenarios on Higgs physics should therefore be distinguishable from the shifts found in the UED model studied here; the direct production of the various new states associated with each model should also assist in distinguishing them.

In summary, the virtual effects of KK excitations in UED can significantly alter Higgs properties which will be measured at future colliders. The implications of radiative corrections in extra-dimensional models have not been studied extensively, primarily because of the resulting divergences. We have shown that in certain scenarios such effects are both calculable and important, and we believe that further investigations along these lines should be undertaken.

Acknowledgements

It is a pleasure to thank C. Anastasiou, J. Hewett, K. Melnikov, and T. Rizzo for many helpful suggestions and conversations. We also thank G. Cacciapaglia, M. Cirelli, and G. Cristadoro for informing us of their results in [34]. This work was supported in part by the National Science Foundation Graduate Research Program.

References

- [1] N. Arkani-Hamed, S. Dimopoulos and G. R. Dvali, Phys. Lett. B **429**, 263 (1998) [arXiv:hep-ph/9803315]; I. Antoniadis, N. Arkani-Hamed, S. Dimopoulos and G. R. Dvali, Phys. Lett. B **436**, 257 (1998) [arXiv:hep-ph/9804398].
- [2] E. Dudas and J. Mourad, Nucl. Phys. B **575**, 3 (2000) [arXiv:hep-th/9911019]; E. Accomando, I. Antoniadis and K. Benakli, Nucl. Phys. B **579**, 3 (2000) [arXiv:hep-ph/9912287]; S. Cullen, M. Perelstein and M. E. Peskin, Phys. Rev. D **62**, 055012 (2000) [arXiv:hep-ph/0001166].
- [3] For an overview of the phenomenology of extra dimensions, see: G. F. Giudice, R. Rattazzi and J. D. Wells, Nucl. Phys. B **544**, 3 (1999) [arXiv:hep-ph/9811291]; T. Han, J. D. Lykken and R. J. Zhang, Phys. Rev. D **59**, 105006 (1999) [arXiv:hep-ph/9811350]; E. A. Mirabelli, M. Perelstein and M. E. Peskin, Phys. Rev. Lett. **82**, 2236 (1999)

- [arXiv:hep-ph/9811337]; J. L. Hewett, Phys. Rev. Lett. **82**, 4765 (1999) [arXiv:hep-ph/9811356]; T. G. Rizzo, Phys. Rev. D **59**, 115010 (1999) [arXiv:hep-ph/9901209].
- [4] I. Antoniadis, Phys. Lett. B **246**, 377 (1990).
- [5] K. R. Dienes, E. Dudas and T. Gherghetta, Phys. Lett. B **436**, 55 (1998) [arXiv:hep-ph/9803466]; Nucl. Phys. B **537**, 47 (1999) [arXiv:hep-ph/9806292].
- [6] N. Arkani-Hamed and S. Dimopoulos, Phys. Rev. D **65**, 052003 (2002) [arXiv:hep-ph/9811353]; N. Arkani-Hamed and M. Schmaltz, Phys. Rev. D **61**, 033005 (2000) [arXiv:hep-ph/9903417].
- [7] K. R. Dienes, E. Dudas and T. Gherghetta, Nucl. Phys. B **557**, 25 (1999) [arXiv:hep-ph/9811428]; N. Arkani-Hamed, S. Dimopoulos, G. R. Dvali and J. March-Russell, Phys. Rev. D **65**, 024032 (2002) [arXiv:hep-ph/9811448].
- [8] K. R. Dienes, E. Dudas and T. Gherghetta, Phys. Rev. D **62**, 105023 (2000) [arXiv:hep-ph/9912455].
- [9] T. Appelquist, H. C. Cheng and B. A. Dobrescu, Phys. Rev. D **64**, 035002 (2001) [arXiv:hep-ph/0012100].
- [10] T. G. Rizzo, Phys. Rev. D **64**, 095010 (2001) [arXiv:hep-ph/0106336]; C. Macesanu, C. D. McMullen and S. Nandi, arXiv:hep-ph/0201300.
- [11] K. Agashe, N. G. Deshpande and G. H. Wu, Phys. Lett. B **514**, 309 (2001) [arXiv:hep-ph/0105084].
- [12] T. Appelquist and B. A. Dobrescu, Phys. Lett. B **516**, 85 (2001) [arXiv:hep-ph/0106140].
- [13] T. Appelquist, B. A. Dobrescu, E. Ponton and H. U. Yee, arXiv:hep-ph/0201131.
- [14] T. Appelquist, B. A. Dobrescu, E. Ponton and H. U. Yee, Phys. Rev. Lett. **87**, 181802 (2001) [arXiv:hep-ph/0107056].
- [15] H. C. Cheng, talk given at the 4th International Workshop On Electron-Electron Interactions At TeV Energies, 7-9 Dec 2001, Santa Cruz, California.

- [16] Gravity contributions to Higgs physics within an effective Lagrangian framework have been discussed in: L. J. Hall and C. Kolda, Phys. Lett. B **459**, 213 (1999) [arXiv:hep-ph/9904236].
- [17] L. Randall and R. Sundrum, Phys. Rev. Lett. **83**, 3370 (1999) [arXiv:hep-ph/9905221].
- [18] J. L. Hewett and T. G. Rizzo, arXiv:hep-ph/0202155.
- [19] M. Masip and A. Pomarol, Phys. Rev. D **60**, 096005 (1999) [arXiv:hep-ph/9902467].
- [20] T. G. Rizzo and J. D. Wells, Phys. Rev. D **61**, 016007 (2000) [arXiv:hep-ph/9906234].
- [21] A. Muck, A. Pilaftsis and R. Ruckl, arXiv:hep-ph/0110391.
- [22] A. Denner, Fortsch. Phys. **41**, 307 (1993).
- [23] G. Passarino and M. J. Veltman, Nucl. Phys. B **160**, 151 (1979).
- [24] H. C. Cheng, B. A. Dobrescu and C. T. Hill, Nucl. Phys. B **573**, 597 (2000) [arXiv:hep-ph/9906327].
- [25] A. Djouadi, M. Spira and P. M. Zerwas, Phys. Lett. B **264**, 440 (1991); S. Dawson, Nucl. Phys. B **359**, 283 (1991).
- [26] R. V. Harlander and W. B. Kilgore, Phys. Rev. D **64**, 013015 (2001) [arXiv:hep-ph/0102241]; arXiv:hep-ph/0201206.
- [27] T. Abe *et al.* [American Linear Collider Working Group Collaboration], in *Proc. of the APS/DPF/DPB Summer Study on the Future of Particle Physics (Snowmass 2001)* ed. R. Davidson and C. Quigg, SLAC-R-570 *Resource book for Snowmass 2001, 30 Jun - 21 Jul 2001, Snowmass, Colorado*.
- [28] P. Nogueira, J. Comput. Phys. **105**, 279 (1993).
- [29] J. A. Vermaseren, arXiv:math-ph/0010025.
- [30] D. Zeppenfeld, arXiv:hep-ph/0203123.
- [31] B. Badelek *et al.* [ECFA/DESY Photon Collider Working Group Collaboration], arXiv:hep-ex/0108012.

- [32] A. Djouadi, V. Driesen, W. Hollik and A. Kraft, Eur. Phys. J. C **1**, 163 (1998) [arXiv:hep-ph/9701342].
- [33] M. Carena, H. E. Haber, H. E. Logan and S. Mrenna, Phys. Rev. D **65**, 055005 (2002) [arXiv:hep-ph/0106116].
- [34] G. Cacciapaglia, M. Cirelli and G. Cristadoro, arXiv:hep-ph/0111287.
- [35] R. Barbieri, L. J. Hall and Y. Nomura, Phys. Rev. D **63**, 105007 (2001) [arXiv:hep-ph/0011311].

Appendix

We present here the Feynman rules involving the $W^{\pm 5(n)}$, which are relevant for the calculations in this paper. All momenta are assumed to flow into the vertices.

$$= 2ie^2 \left\{ 1, -\frac{c_W}{s_W} \right\} g_{\mu\nu}$$

$$= -ie \left\{ 1, -\frac{c_W}{s_W} \right\} (p_1 - p_2)_\mu$$

$$= \mp m_n \left\{ 1, -\frac{c_W}{s_W} \right\} g_{\mu\nu}$$

$$= -i \frac{e}{s_W} M_W$$

$$= \mp \frac{e}{2s_W} m_n$$